Evolution of collectivity in the $N = 100$ isotones near ^{170}Yb

V. Karayonchev,* J.-M. Régis, J. Jolie, A. Blazhev, R. Altenkirch, S. Ansari, M. Dannhoff, F. Diel, A. Esmaylzadeh, C. Fransen, R.-B. Gerst, K. Moschner, C. Müller-Gatermann, N. Saed-Samii, S. Stegemann, N. Warr, and K. O. Zell
Institut für Kernphysik, Universität zu Köln, D-50937 Köln, Germany
(Received 28 November 2016; published 21 March 2017)

An experiment using the electronic $\gamma - \gamma$ fast-timing technique was performed to measure lifetimes of the yrast states in ^{170}Yb. The lifetime of the yrast 2^+ state was determined using the slope method. The value of $\tau = 2.33(3)$ ns is in good agreement with the lifetimes measured using other techniques. The lifetimes of the first 4^+ and 6^+ states are determined using the generalized centroid difference method. The derived $B(E2)$ values are compared to calculations done using the confined beta soft model and show good agreement with the experimental values. These calculations were extended to the isotonic chain $N = 100$ around ^{170}Yb and show a good quantitative description of the collectivity observed along it.

DOI: 10.1103/PhysRevC.95.034316

I. INTRODUCTION

Shape phase transition is a common phenomenon in many physical systems including the atomic nucleus [1]. A prime example is the transition of the nuclear shape from a spherical to a rigidly deformed ellipsoidal one. An adequate description of the quadrupole collective excitation of even-even nuclei in this shape changing region can be achieved in the framework of the Bohr Hamiltonian [2]

$$H_B = -\frac{\hbar^2}{2B}\left[\frac{1}{\beta^4}\frac{\partial}{\partial\beta}\beta^4\frac{\partial}{\partial\beta} + \frac{1}{\beta^2}\frac{1}{\sin 3\gamma}\frac{\partial}{\partial\gamma}\sin 3\gamma\frac{\partial}{\partial\gamma} + \frac{1}{4\beta^2}\sum_k \frac{Q_k^2}{\sin^2\left(\gamma - \frac{2}{3}\pi k\right)}\right] + V(\beta,\gamma). \quad (1)$$

By choosing a proper potential $V(\beta,\gamma)$ for the quadrupole degrees of freedom β and γ, both the spherical and the rigidly deformed nuclei can be described as an analytic solution of this Hamiltonian. In 2001, Iachello developed an approximate solution for the Bohr Hamiltonian H_B, known as the X(5) symmetry [3], which aims at describing analytically nuclei near the critical point of the shape phase transition. The potential used in this solution is separable of the form $V(\beta,\gamma) = u(\beta) + v(\gamma)$, assuming a harmonic oscillator potential in γ with a minimum at $\gamma = 0^0$ and an infinite square well for β with one of the walls located at 0 and the other at some finite value β_M [Fig. 1(a)]. This relatively simple model was confirmed in the $N = 90$ isotones [4–6] and led to many experimental searches [7–14]. The situation further improved in 2004 when Pietralla and Gorbachenko generalized this solution for the transition region from the X(5) symmetry ($R_{4/2} = 2.91$) to the rigid-rotor solution ($R_{4/2} = 3.33$), a solution known as the confined beta soft (CBS) model [15]. The potential $v(\beta)$ is modified by moving one of the walls of the square well from zero to some value $\beta_m = r_\beta\beta_M$, where $r_\beta \in [0,1)$ [Fig. 1(b)], while the potential in γ remains the same as in the X(5) case. With this definition of r_β the CBS model reproduces the X(5) solution when $r_\beta = 0$ and the rigid rotor when $r_\beta \to 1$ [see Fig. 1(c)]. By increasing r_β the stiffness of the potential increases limiting the quantum fluctuation of the deformation parameter β. In such a way the degree of the so-called centrifugal stretching is controlled and all the values of the $R_{4/2}$ parameter between 2.91 and 3.33 can be reproduced by choosing a proper value of r_β.

Of particular interest is the isotonic chain $N = 100$ from ^{168}Er($R_{4/2} = 3.31$), which represents a solution close to the rigid rotor solution, toward ^{176}Os which has been reported as having an X(5) symmetry [8]. By using r_β as an evolution parameter, the CBS model can be tested for this chain of isotones. The lifetimes of the yrast-band states within this isotonic chain were known up to spin 6 with the exception of the ^{170}Yb nucleus where the lifetimes of the 4^+ and the 6^+ states were unknown. Measuring the lifetimes of these states completes the systematics in this isotonic chain, which makes it possible to test of the CBS model for the whole chain of isotones and assess how well it is able to account for the evolution of energies and the reduced transition probabilities observed in the ground-state band of these nuclei.

II. EXPERIMENT AND ANALYSIS

To determine the unknown lifetimes of the first excited 4^+ and 6^+ states in ^{170}Yb, an experiment was performed at the Institute for Nuclear Physics at the University of Cologne. The nucleus of interest was populated in the ^{168}Er$(\alpha,2n)^{170}$Yb fusion-evaporation reaction. An average beam current of 10 pnA with an energy of 27 MeV was provided by the Cologne 10 MV FN-Tandem accelerator. The γ rays produced in the reaction were measured using a mixed detector array consisting of 8 HPGe detectors and 8 $LaBr_3$(Ce) (called hereafter "LaBr") detectors placed inside the HORUS spectrometer [16]. Six of the LaBr detectors were placed inside bismuth germanate (BGO) Compton shields to suppress the Compton background. The background from scattered γ rays was further reduced by lead collimators and/or lead shields around the detectors. Background reduction is of key importance since it is time correlated and causes a major systematic error in the measurements of the lifetimes done by using the fast-timing technique [17]. The time difference

*karayon@ikp.uni-koeln.de

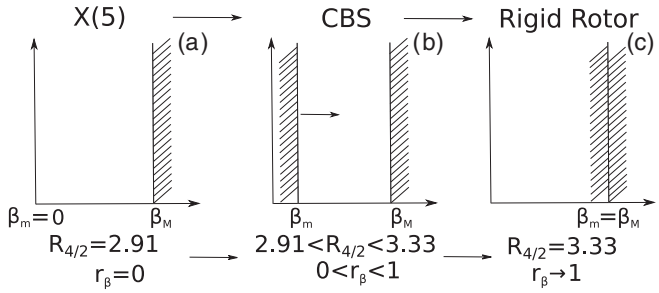

FIG. 1. Form of the potential $\nu(\beta)$ for (a) X(5), (b) CBS, and (c) rigid rotor.

spectra of every unique combination of LaBr detectors were recorded by time to amplitude converters (TAC) applying the method described by the authors of Ref. [18]. The detector energy signals and the TAC amplitudes were recorded using 80 MHz synchronized digitizers. The data were stored in a "listmode" data format. In such a way, it is possible to sort double and triple coincidences off-line, which are used for further data analysis of the experiment. A partial level scheme of the ground-state band of the ^{170}Yb nucleus, relevant for this experiment, is shown in Fig. 2(a). In the same figure, gated spectra of the HPGe and the LaBr detectors are presented showing the cleanliness of the $(\alpha,2n)$ reaction.

By applying two energy gates on the LaBr detectors, a feeder-decay cascade corresponding to a given state of interest can be selected. For every combination of LaBr detectors the setup provides two independent time difference spectra, the delayed and the antidelayed, measured as the time difference between a start and a stop detector. The delayed spectrum is produced when the feeding transition provides the start signal and the decay transition the stop signal. The antidelayed spectrum is produced when the decay transition provides the start signal and the feeding transition the stop signal.

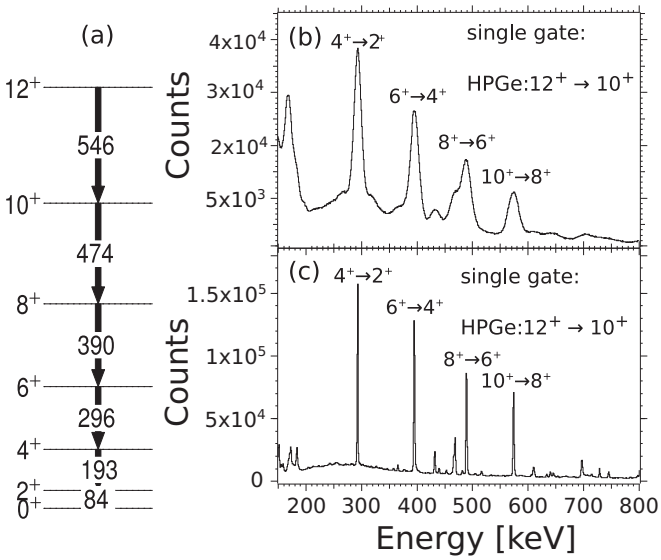

FIG. 2. (a) Partial level scheme of the ground-state band of ^{170}Yb. (b) Single-gated LaBr spectrum. (c) Single-gated HPGe spectrum.

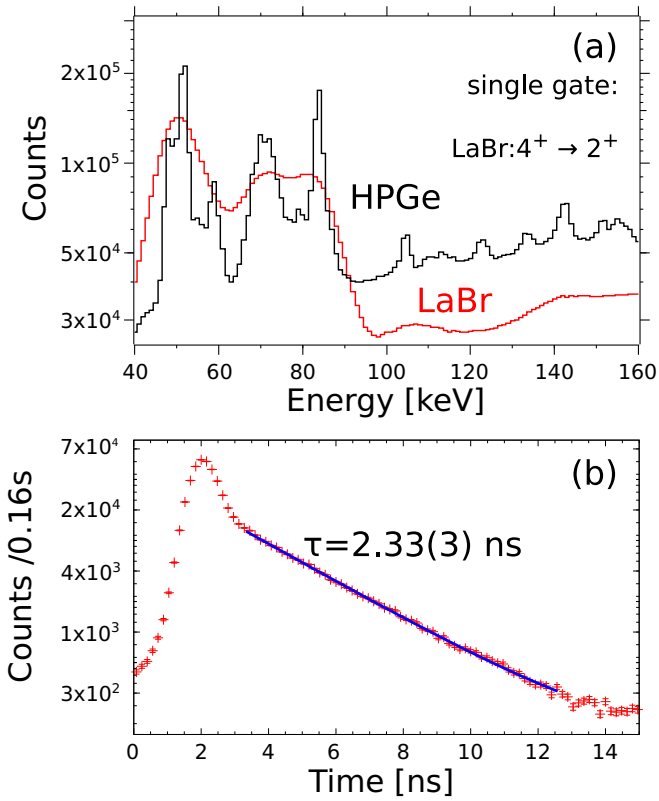

FIG. 3. (a) HPGe-LaBr and LaBr-LaBr coincidence spectra. (b) Time-difference spectrum (see text for details). The line indicates the fit to the data used to extract the lifetime.

In the simple case where no background is present, the delayed time spectrum $D_d(t)$ is given as the convolution of the prompt response function (PRF) of the setup with an exponential decay

$$D_d(t) = \frac{1}{\tau} N_0 \int_{-\infty}^{t} \mathrm{PRF}(t') e^{-\frac{(t-t')}{\tau}} dt', \tag{2}$$

where τ is the lifetime associated with the feeder-decay combination and N_0 is the total number of the counts in the time spectrum. The PRF describes the zero time response of the setup. The antidelayed time spectrum $D_a(t)$ is obtained by inverting the time in this equation, which is equivalent to reversing the energy gates set on the LaBr detectors.

Depending on the lifetime of interest, two methods can be used to analyze the time-difference spectra. If $\tau >$ FWHM(PRF), the time spectra become asymmetric and a slope appears on one side of the spectra. Fitting an exponential decay to this slope yields the lifetime of interest. If $\tau \lesssim$ FWHM(PRF), the recently developed generalized centroid difference (GCD) method [19], an extension to the centroid shift method [20], can be used to extract the lifetime. The centroid $C(D)$ is defined as the first moment of the time distribution $D(t)$

$$C(D(t)) = \langle t \rangle = \frac{\int_{-\infty}^{\infty} t D(t) dt}{\int_{-\infty}^{\infty} D(t) dt} \tag{3}$$

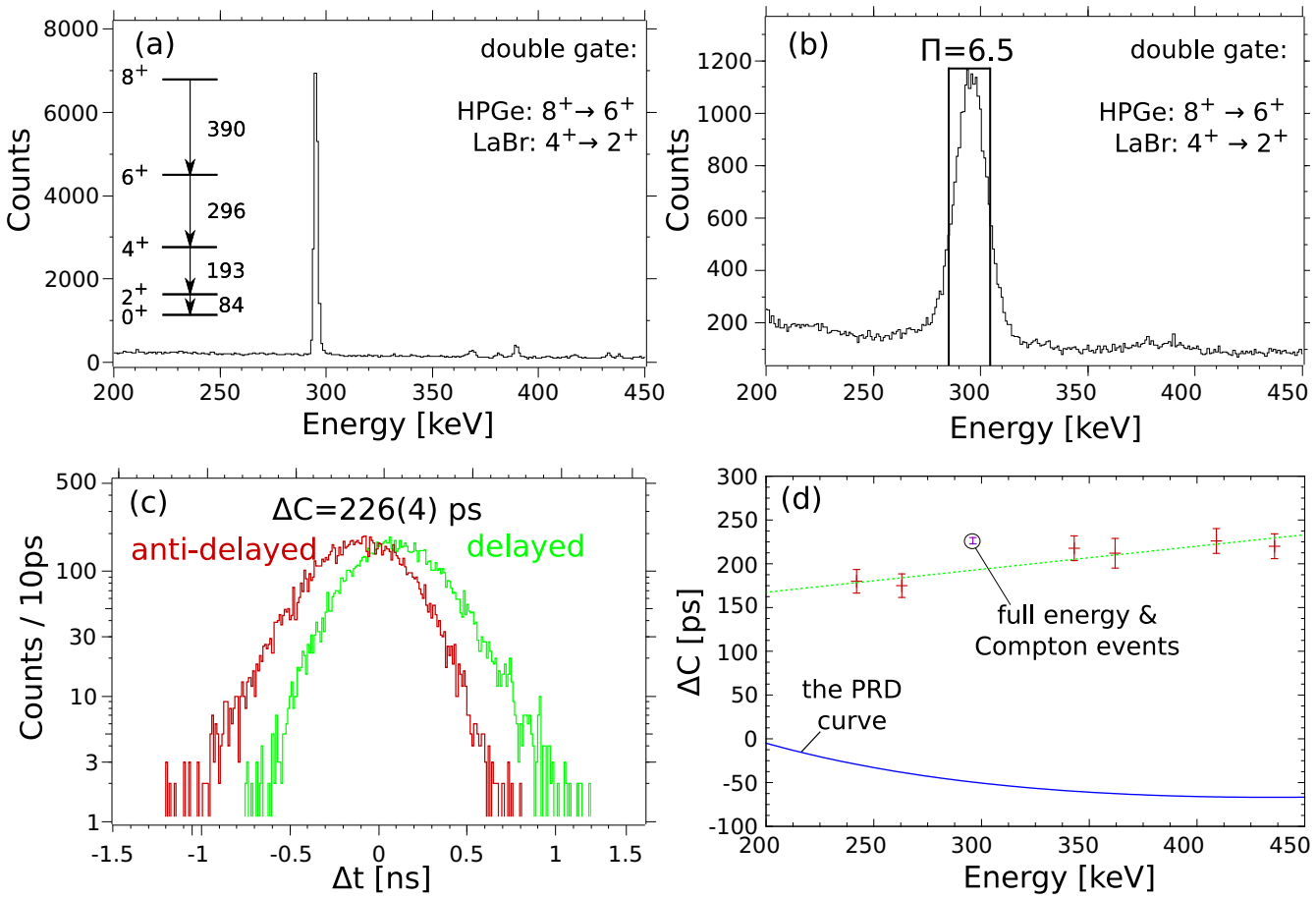

FIG. 4. The figure indicates the basic steps for extracting the lifetime of the first excited 4^+ state. (a) HPGe detector projection in HPGe-LaBr gates used to check for unwanted transitions. (b) LaBr detector projection in HPGe-LaBr gates indicating the gate used to produce the time-difference spectra and the corresponding peak-to-background ratio Π for the gate region. (c) Time-difference spectra for 293–193 keV feeder-decay combination. (d) The fitted time response of the background (dashed line), together with the PRD curve and the obtained centroid difference from (c).

with the statistical error given by the variance of $D(t)$

$$\delta C = \sqrt{\mathrm{Var}[D(t)]} = \sqrt{\langle t^2\rangle - \langle t\rangle^2}. \tag{4}$$

According to the GCD method, the centroid of the delayed time distribution is displaced from the centroid of the antidelayed time distribution by two times the mean lifetime τ plus an energy dependent $\gamma - \gamma$ time-walk correction, known as a prompt response difference (PRD)

$$C(D(t)_d) - C(D(t)_a) = \Delta C = 2\tau + \mathrm{PRD}. \tag{5}$$

The energy dependency of the PRD has to be determined experimentally.

The procedures described above have to be carried out for all the detector combinations, which in the case of 8 LaBr detectors, are 28 combinations. The main idea behind the GCD method is that, instead of doing this procedure for every single combination, one can superimpose all the delayed and all the antidelayed time spectra without any corrections (for a detailed explanation see Ref. [18]). Then Eq. (5) can be generalized for the whole fast-timing detector array.

III. RESULTS

The first excited 2^+ state of ^{170}Yb at 84 keV is fed by the 193-keV transition. As this state has a lifetime in the ns range, the slope method is used. Single-gated HPGe and LaBr detector spectra are shown in Fig. 3(a). By putting an additional gate at 84 keV on the LaBr detector energy, as indicated in the figure, the delayed and the antidelayed time spectra are produced. The antidelayed time spectrum is inverted and translated on top of the delayed spectra. The sum of these spectra is shown in Fig. 3(b). There are two components in this spectrum. The short-lived component caused by the background, which is mainly due to Compton events and lead x rays which form a doublet with the 84-keV transition. The long-lived component is due to the lifetime of the 2^+ state. An exponential fit with a constant background to this data yields the lifetime of 2.33(3) ns. The error indicated is the combined error of the systematic error that arises when choosing the fit region and the value of the constant background and the statistical error obtained when fitting the lifetime.

Both lifetimes of the first excited 4^+ and 6^+ states are short compared to the FWHM of the PRF and were determined using the GCD method. To perform this measurement, a calibration

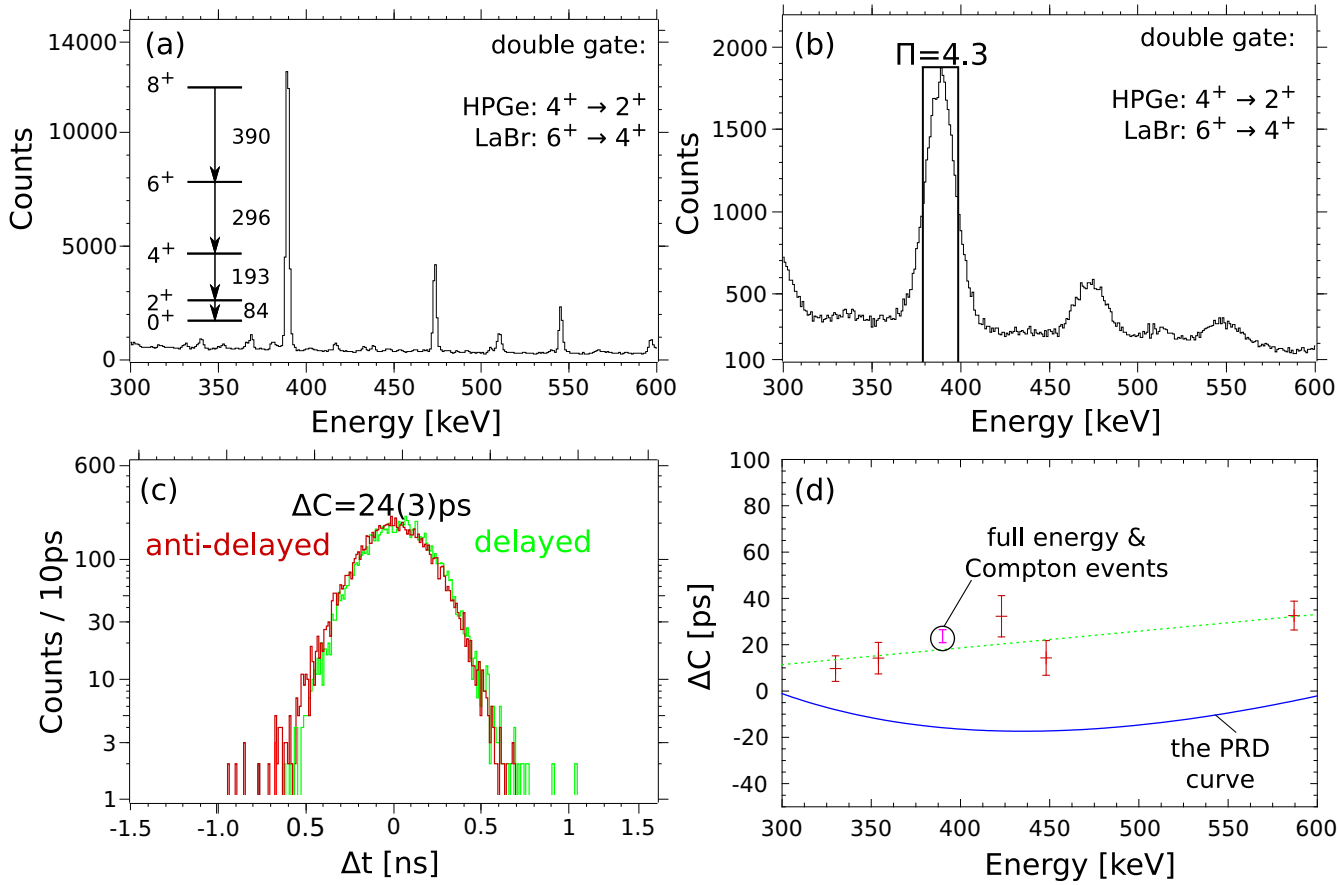

FIG. 5. Same as Fig. 4, but for the first excited 6^+ state. The tail observed around 300 keV in (b) is coming from a peak located at 296 keV. This peak is due to coincidences with the Compton background in the LaBr gate.

of the PRD curve is necessary. This is done by a standard calibration procedure using a ^{152}Eu calibration source [18]. Selecting a proper feeder-decay combination for a state with known lifetime within the decay products of the source, the centroid difference is obtained and using Eq. (5) the PRD is obtained. The points are fitted with the function [18]

$$\frac{a}{\sqrt{E_\gamma + b}} + cE_\gamma + d. \tag{6}$$

The uncertainty of the PRD curve is defined as the statistical 2σ deviation of the data from the fitted curve corresponding to 6 ps.

To extract the lifetimes of first excited 4^+ and 6^+ states, triple γ coincidences were used to obtain the time difference spectra. By putting an additional gate on the HPGe detectors the background level is significantly reduced. Doubly gated HPGe, LaBr spectra are shown in Figs. 4(a) and 4(b). The high-energy resolution of the HPGe detectors also allows one to ensure that there are no undesired transitions with energies similar to that of the $6^+ \rightarrow 4^+$ transition, which cannot be distinguished by the low-resolution LaBr detectors and might provide a systematic error. By applying a second gate in the LaBr detectors the delayed and the antidelayed time spectra are produced and shown in Fig. 4(c). Measuring the centroid difference ΔC between them and using Eq. (5), the value of $\tau = 138(5)$ ps is obtained. Even though the energy spectra are very clean, with a peak-to-background ratio of 6.5 for the LaBr detectors, there is still some background seen under the full-energy peak. These background events also contribute to the time spectra shown in Fig. 4(c). To have a precise lifetime measurement, this contribution has to be determined and a correction needs to be applied. This is done by putting gates on the background region around the full-energy peak to obtain the time response of the background (the centroid difference) ΔC_{bg} and interpolate this response to the position of the full-energy peak (FEP). Knowing the time response of the background at the position of the full-energy peak, the measured centroid difference ΔC is corrected in the following way [18]:

$$\Delta C_{\mathrm{FEP}} = \Delta C + \frac{\Delta C - \Delta C_{bg}}{\Pi}, \tag{7}$$

where Π is the peak-to-background ratio in the energy-gated LaBr spectrum used when ΔC was determined. This leads to the following formula for the lifetime:

$$\tau = \frac{1}{2}\left(\Delta C + \frac{\Delta C - \Delta C_{bg}}{\Pi} - \mathrm{PRD}\right). \tag{8}$$

TABLE I. Measured lifetime in the yrast band of ^{170}Yb and the feeder and decay energies used to obtain the time-difference spectra. Adopted literature values taken from Ref. [21] are given for a comparison.

state	E_{feeder} [keV]	E_{decay} [keV]	HPGe gate [kev]	τ (exp.) [ps]	τ(lit.) [ps]
2^+	193	84	–	2330(30)	2316(19)[a]
4^+	296	193	390 & 474	141(5)	–
6^+	390	296	193 & 474	19(4)	–
8^+	474	390	193 & 296	<6	4.28(36)[b]

[a]Weighted average from Refs. [22–24], adopted in Ref. [21].
[b]Reference [25], adopted in Ref. [21].

Using this correction for the background, we obtain the the final value of $\tau(4^+) = 141(5)$ ps. The error of the lifetime follows from error propagation.

A complementary measurement of this lifetime was performed by changing the gate in the HPGe detector to the $10^+ \rightarrow 8^+$ transition energy. This independent measurement gives the result of $\tau(4^+) = 141(6)$ ps, which agrees precisely with the previous measurement but has a higher statistical error due to the lower efficiency of the HPGe detectors at higher energies and the lower population of the 10^+ state as compared to the 8^+ state.

By using appropriate gates the same analysis was performed for the first excited 6^+ state. The resulting lifetime is $\tau(6^+) = 19(4)$ ps. The corresponding figures are presented in Fig. 5. The lifetime of the first excited 8^+ state is already at the limit of the applicability of the GCD method and only an upper limit of 6 ps could be determined.

The results obtained are summarized in Table I together with the adopted literature values. The measured lifetime of the 2^+ state agrees with the adopted literature value of 2316(19) ps which was determined as a weighted average of three experiments done using the fast-timing technique in the β^- decay of ^{170}Tm [22–24]. The upper limit for the 8^+ state lifetime from this work is also consistent with the literature value of 4.28(36) ps, which was determined in a DSAM measurement [25]. With the newly obtained lifetimes, the reduced transition probabilities $B(E2)$ are calculated and the result is presented in Table II.

TABLE II. Calculated reduced transition probabilities in ^{170}Yb. The values in boldface are obtained in the experiment. The conversion coefficients α used in the calculation are obtained from the code BrIccFo [26].

Transition	E_{decay} [keV]	$B(E2)$(CBS) [W.u.]	$B(E2)$(exp.) [W.u.]	α
$2^+ \rightarrow 0^+$	84	202	**203(4)**	6.28(9)
$4^+ \rightarrow 2^+$	193	292	**297(11)**	0.302(5)
$6^+ \rightarrow 4^+$	296	329	**316(66)**	0.077(1)
$8^+ \rightarrow 6^+$	390	355	367(11)[a]	0.0345(6)
$10^+ \rightarrow 8^+$	474	378	359 (26)[a]	0.0205(3)

[a]From Ref. [25].

IV. DISCUSSION

The solution of the Bohr Hamiltonian [Eq. (1)] with a CBS potential is done by assuming a decoupling of the quadrupole degrees of freedom β and γ. The wave functions can then be written as $\Psi(\beta,\gamma,\theta_i) = \xi_L(\beta)\eta_K(\gamma)D^L_{M,K}(\theta_i)$, where $D^L_{M,K}(\theta_i)$ are the Wigner functions with θ_i defining the orientation of the intrinsic system and $\eta_K(\gamma)$ is taken from Ref. [3]. The function $\xi_K(\gamma)$ satisfies the radial differential equation

$$\left[-\frac{1}{\beta^4}\frac{\partial}{\partial\beta}\beta^4\frac{\partial}{\partial\beta}\frac{1}{4\beta^2}\frac{4}{3}L(L+1)+u(\beta)\right]\xi_L(\beta) = \epsilon_\beta\xi_L(\beta). \tag{9}$$

After applying proper quantisation conditions, the solutions of this equation are given by [3]

$$\xi_{L,s}(\beta) = c_{L,s}\beta^{-3/2}\left[J_\nu\left(z^{r_\beta}_{L,s}\frac{\beta}{\beta_M}\right) - \frac{J_\nu\left(r_\beta z^{r_\beta}_{L,s}\right)}{Y_\nu\left(r_\beta z^{r_\beta}_{L,s}\right)}Y_\nu\left(z^{r_\beta}_{L,s}\frac{\beta}{\beta_M}\right)\right], \tag{10}$$

with normalization

$$\frac{1}{c^2_{L,s}} = \int_{\beta_m}^{\beta_M}\beta^4[\xi_{L,s}(\beta)]d\beta \tag{11}$$

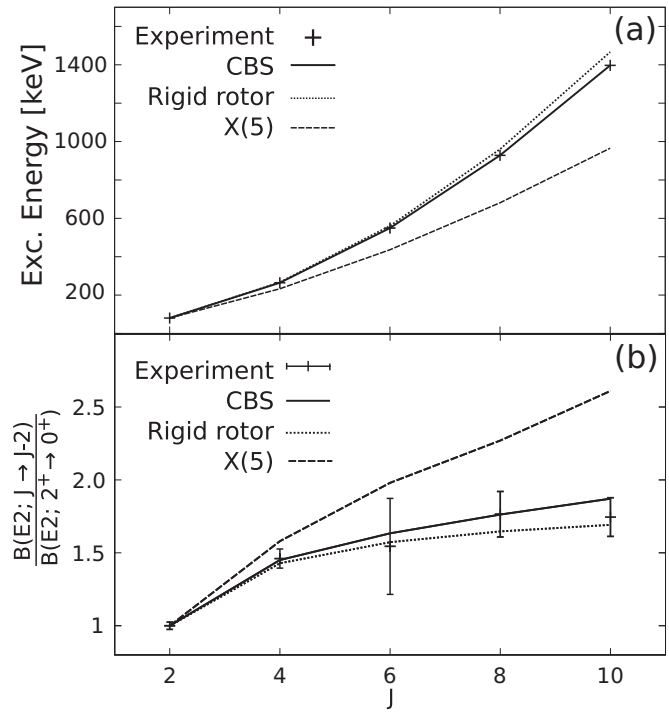

FIG. 6. (a) Excitation energies and (b) reduced tranistion probabilities of the ground-state-band levels as function of the spin J compared to the CBS prediction. The X(5) and the rigid rotor solutions are also shown as dashed and dotted lines, respectively. Data for the first excited 2^+, 4^+, and 6^+ states are from this experiment and for the 8^+ and 10^+ states from Ref. [25].

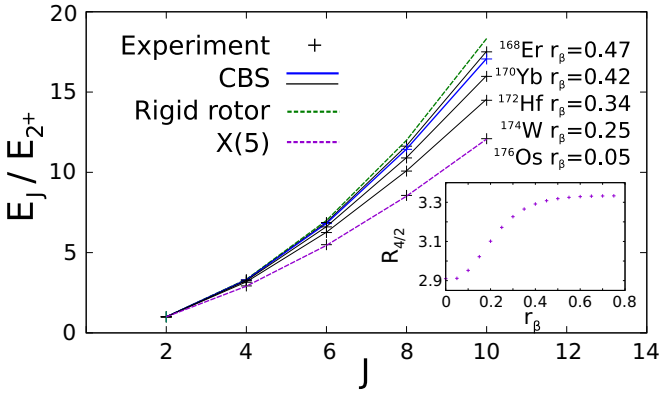

FIG. 7. The excitation energies of the ground-band states for the isotonic chain from ^{168}Er to ^{176}Os normalized to the 2^+ state energy. The values of the parameter r_β, controlling the energies within the CBS model for the different isotones, are also indicated. Data are taken from Refs. [21,30–33]. The inset shows the $R_{4/2}$ value dependence on r_β.

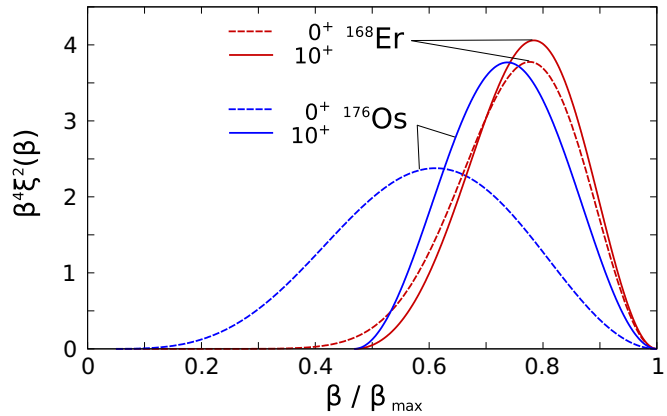

FIG. 8. CBS wave function densities for the first excited 0^+ and 10^+ states in ^{168}Er and ^{176}Os.

and eigenvalues

$$E_{L,s} = \frac{\hbar^2}{2B\beta_M}\left(z_{L,s}^{r_\beta}\right)^2. \tag{12}$$

Here, the concept of centrifugal stretching, which is a phenomenon that has been reported in the midshell rare-earth region [27–29], arises naturally from the properties of the wave functions $\xi_{L,s}(\beta)$. As the angular momentum L increases, the density of the wave function is pushed to higher values of β. Since β defines the degree of quadrupole deformation, this increase would result in an elongation of the nuclear shape and an increase of the moment of inertia B of the nucleus. This would lead to a deviation of the rigid rotor behavior, where the moment of inertia is fixed and the energies for the ground-state band are given by the simple relation $E_L = (\hbar^2/2B_{\text{const}})L(L+1)$ and $R_{4/2}$ has a fixed value of 3.33. The energies of the ground state band in ^{170}Yb together with the CBS fit are shown in Fig. 6(a). Even though this nucleus has a $R_{4/2}$ parameter of 3.30, which puts it very close to the rigid rotor, some centrifugal stretching is still observed and the CBS model can account for it very accurately. The dependence of $R_{4/2}$ on r_β is given in the inset of Fig. 7. By using $r_\beta = 0.419$, the CBS model is able to reproduce the energies of the yrast band up to spin 10 within a 1 keV margin (see Table III). The rigid rotor and the X(5) solutions are given in the same figure for comparison as they represent the limits of the model.

The reduced transition probabilities within the framework of the CBS model are calculated by using the leading order quadrupole transition operator [15]

$$\hat{T} = e_{\text{eff}}\hat{\beta}$$
$$\text{with } e_{\text{eff}} = \frac{3}{4\pi}\beta_M Z R_0^2 e^{\frac{2}{3}\ln A}, \tag{13}$$

where $R_0 = 1.22$ fm. The results for the normalized $B(E2)$ values which depend only on r_β are compared to the experimental values in Fig. 6(b). It can be seen that the normalized $B(E2)$ values are reproduced by the CBS model within the experimental errors up to spin 10. Due to the rather large experimental uncertainties, it is not possible to distinguish whether the ^{170}Yb is a CBS-rotor or a rigid rotor solely from the transition probabilities.

The calculations done for the ^{170}Yb nucleus can be extended to the isotonic chain from ^{168}Er to ^{176}Os using r_β as an evolution parameter. By choosing proper values of the parameter r_β the different amounts of centrifugal stretching, as seen in Fig. 7, observed in the nuclei can be described. The $R_{4/2}$ value is directly linked to the centrifugal stretching and it depends only on r_β. This dependence is given in the inset of Fig. 7. The values of r_β vary between 0.47 for the case of

TABLE III. Adopted ground state band energies in the $N = 100$ isotonic chain from ^{168}Er to ^{176}Os are compared to the CBS model calculations. The parameter r_β together with an additional scaling parameter are used in the minimisation procedure. In addition the rigid rotor and X(5) model predictions are given for the ^{168}Er and the ^{176}Os nuclei as these solutions represent the two limits of the CBS model. All energies are in keV. Data used are taken from Nuclear Data Sheets [21,30–33].

State	^{168}Er		CBS	^{170}Yb		^{172}Hf		^{174}W		CBS	^{176}Os	X(5)
	Rotor	Expt.		CBS	Expt.	CBS	Expt.	CBS	Expt.		Expt.	
2^+	80	80	80	84	84	95	95	113	113	136	135	135
4^+	266	264	264	277	277	309	309	357	356	395	396	393
6^+	589	549	549	573	573	629	628	706	706	739	743	736
8^+	957	928	928	963	963	1037	1038	1137	1139	1155	1157	1150
10^+	1463	1397	1397	1437	1437	1521	1521	1639	1638	1639	1634	1631

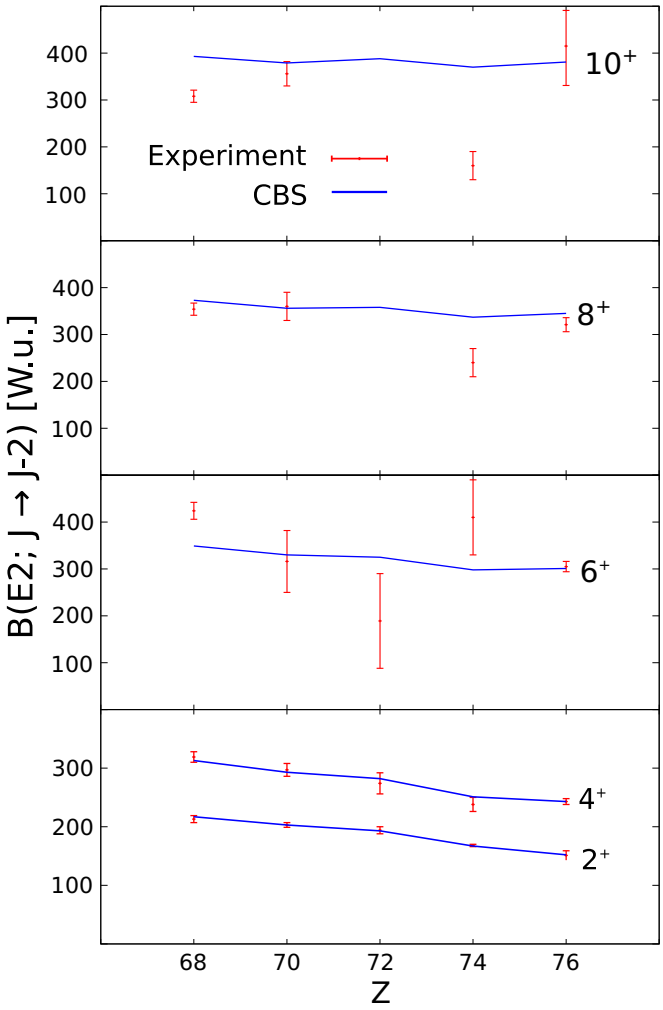

FIG. 9. Evolution of the reduced transition probabilities for the yrast states up to spin 10 within the isotonic chain from ^{168}Er to ^{176}Os. The values of the parameter β_M are 0.45, 0.44, 0.43, 0.37, and 0.41, respectively. Data for ^{172}Hf are taken from Ref. [34], for the 2^+ state in ^{174}W from Ref. [35] and all the rest from Nuclear Data Sheets [21,30–33].

^{168}Er, where the potential on β is very stiff and the degree of centrifugal stretching is small, to 0.05 for ^{176}Os where a large degree of centrifugal stretching is observed, see Fig. 7. This effect can be easily understood by looking at the wave function density $\beta^4\xi^2(\beta)$ given in Fig. 8. It can be seen that while the center of gravity of the CBS wave function for the ground-band states of ^{176}Os shifts significantly as the spin increases from 0 to 10, this shift is very small in the case of ^{168}Er. The results of the calculations for the absolute energies for the isotonic chain from ^{168}Er to ^{176}Os are shown in Table III. Overall, the model is able to describe all the energies of the yrast states up to spin 10 very well with accuracy of better than 2 keV. In the case of ^{176}Os, the CBS prediction for the excitation energies starts to deviate from the experimental values, especially for the higher spins. This is most probably due to the fact that the assumption of having a vertical wall at β_M in potential on β is too naive, while a more realistic potential would have the form given in Fig. 1 in Ref. [3].

The model is also able to account for the evolution of the observed reduced transition probabilities $B(E2)$ within the yrast bands of the nuclei in the isotonic chain. To reproduce the absolute transition probabilities the parameter β_M has to be used also in the minimization procedure, as the quadrupole operator $\hat{T}$ is proportional to β_M [see Eq. (13)]. The experimental $B(E2)$ values for the nuclei in the chain together with the CBS calculations are presented in Fig. 9. The values of the β_M parameter are given in the caption of this figure. As expected, the $B(E2)$ values smoothly increase as N approaches midshell. The CBS model is able to account for this evolution reproducing all the reduced transition probabilities of the first excited 2^+ and the 4^+ states within the experimental uncertainties. There is a good agreement for both the ^{170}Yb and ^{176}Os nuclei for all the yrast states up to spin 10, however, the agreement for other nuclei is sporadic.

V. CONCLUSION

Using the fast-timing technique, the lifetimes of the yrast 4^+ and 6^+ states in ^{170}Yb have been determined. With the newly obtained data we were able to test the CBS model for both the transition probabilities and the excitation energies of the yrast band up to spin 10. The performed calculations are in a good agreement with the experimental data. By measuring these lifetimes, the systematics of the reduced transition probabilities of the first three excited states of the nuclei in the $N = 100$ isotonic chain from ^{168}Er to ^{176}Os has been completed. CBS calculations were done for all even-even nuclei in the isotonic chain. The model is able to describe the excitation energies very well due to its ability to account for the different degrees of centrifugal stretching observed in the nuclei. For the evolution of the reduced transition probabilities, we are able to reach a qualitative description for the lowest excited states.

ACKNOWLEDGMENTS

The authors would like to thank Norbert Pietralla from TU Darmstadt and Georgi Rainovski from Sofia University for the helpful discussions during the preparation of this manuscript. This work was supported by the Deutsche Forschungsgemeinschaft (DFG) under Grant No. JO 391/16-1.

[1] P. Cejnar, J. Jolie, and R. F. Casten, Rev. Mod. Phys. **82**, 2155 (2010).
[2] A. Bohr, Kong. Dansk. Vid. Selsk **26**, 14 (1952).
[3] F. Iachello, Phys. Rev. Lett. **87**, 052502 (2001).
[4] R. F. Casten and N. V. Zamfir, Phys. Rev. Lett. **85**, 3584 (2000).
[5] R. Krücken, B. Albanna, C. Bialik, R. F. Casten, J. R. Cooper, A. Dewald, N. V. Zamfir, C. J. Barton, C. W. Beausang, M. A. Caprio, A. A. Hecht, T. Klug, J. R. Novak, N. Pietralla, and P von Brentano, Phys. Rev. Lett. **88**, 232501 (2002).

[6] D. Tonev, A. Dewald, T. Klug, P. Petkov, J. Jolie, A. Fitzler, O. Möller, S. Heinze, P. von Brentano, and R. F. Casten, Phys. Rev. C **69**, 034334 (2004).
[7] E. A. McCutchan, N. V. Zamfir, M. A. Caprio, R. F. Casten, H. Amro, C. W. Beausang, D. S. Brenner, A. A. Hecht, C. Hutter, S. D. Langdown, D. A. Meyer, P. H. Regan, J. J. Ressler, and A. D. Yamamoto, Phys. Rev. C **69**, 024308 (2004).
[8] A. Dewald *et al.*, J. Phys. G **31**, S1427 (2005).
[9] D. L. Balabanski *et al.*, Int. J. Mod. Phys. E **15**, 1735 (2006).
[10] X. Hao, L. H. Zhu, X. G. Wu, G. S. Li, B. Pan, L. L. Wang, Y. Zheng, L. Wang, X. Q. Li, Y. Liu, H. B. Ding, and Z. Y. Li, Chinese Phys. C **33**, 151 (2009).
[11] P. G. Bizzeti, A. M. Bizzeti-Sona, D. Tonev, A. Giannatiempo, C. A. Ur, A. Dewald, B. Melon, C. Michelagnoli, P. Petkov, D. Bazzacco, A. Costin, G. deAngelis, F. DellaVedova, M. Fantuzi, E. Farnea, C. Fransen, A. Gadea, S. Lenzi, S. Lunardi, N. Marginean, R. Marginean, R. Menegazzo, D. Mengoni, O. Moller, A. Nannini, D. R. Napoli, M. Nespolo, P. Pavan, A. Perego, C. M. Petrache, N. Pietralla, C. RossiAlvarez, and P. Sona, Phys. Rev. C **82**, 054311 (2010).
[12] X. Hao, L. H. Zhu, X. G. Wu, C. Y. He, B. Pan, Y. Zheng, L. L. Wang, L. Wang, X. Q. Li, Y. Liu, H. B. Ding, Z. Y. Li, J. F. Zhang, H. B. Sun, and G. S. Li, J. Phys. G **38**, 025102 (2011).
[13] P. Petkov, K. A. Gladnishki, A. Dewald, C. Fransen, M. Hackstein, J. Jolie, Th. Pissulla, W. Rother, and K. O. Zell, J. Phys.: Conf. Series **366**, 012036 (2012).
[14] M. G. Procter *et al.*, J. Phys.: Conf. Series **381**, 012062 (2012).
[15] N. Pietralla and O. M. Gorbachenko, Phys. Rev. C **70**, 011304 (2004).
[16] A. Linnemann, Ph.D. thesis, Universität zu Köln, 2006.
[17] J.-M. Régis, M. Dannhoff, J. Jolie, C. Müller-Gatermann, and N. Saed-Samii, Nucl. Instrum. Methods Phys Res., Sec. **811**, 42 (2016).
[18] J.-M. Régis, N. Saed-Samii, M. Rudigier, S. Ansari, M. Dannhoff, A. Esmaylzadeh, C. Fransen, R.-B. Gerst, J. Jolie, V. Karayonchev, C. Müller-Gatermann, and S. Stegemann, Nucl. Instrum. Methods Phys Res., Sect. **823**, 72 (2016).
[19] J.-M. Régis *et al.*, Nucl. Instrum. Methods Phys. Res., Sect. **726**, 191 (2013).
[20] Z. Bay, Phys. Rev. **77**, 419 (1950).
[21] C. M. Baglin, Nucl. Data Sheets **96**, 611 (2002).
[22] M. I. Green, P. F. Kenealy, and G. B. Beard, Nucl. Instrum. Methods **99**, 445 (1972).
[23] D. K. Gupta and G. N. Rao, Nucl. Phys. A **182**, 669 (1972).
[24] A. Backlin, S. G. Malmskog, and H. Solhed, Arkiv Fysik **34**, 495 (1967).
[25] F. Kearns, G. Varley, G. D. Dracoulis, T. Inamura, J. C. Lisle, and J. C. Willmott, Nucl. Phys. A **278**, 109 (1977).
[26] T. Kibédi, T. W. Burrows, M. B. Trzhaskovskaya, P. M. Davidson, and C. W. Nestor Jr., Nucl. Instrum. Methods Phys. Res., Sect. **589**, 202 (2008).
[27] S. C. K. Nair and A. Ansari, Phys. Lett. B **47**, 200 (1973).
[28] A. Costin, M. Reese, H. Ai, R. F. Casten, K. Dusling, C. R. Fitzpatrick, G. Gürdal, A. Heinz, E. A. McCutchan, D. A. Meyer, O. Möller, P. Petkov, N. Pietralla, J. Qian, G. Rainovski, and V. Werner, Phys. Rev. C **79**, 024307 (2009).
[29] M. K. Smith, V. Werner, J. R. Terry, N. Pietralla, P. Petkov, Z. Berant, R. J. Casperson, A. Heinz, G. Henning, R. Lüttke, J. Qian, B. Shoraka, G. Rainovski, E. Williams, and R. Winkler, Phys. Rev. C **87**, 044317 (2013).
[30] C. M. Baglin, Nucl. Data Sheets **111**, 1807 (2010).
[31] B. Singh, Nucl. Data Sheets **75**, 199 (1995).
[32] E. Browne and H. Junde, Nucl. Data Sheets **87**, 15 (1999).
[33] M. S. Basunia, Nucl. Data Sheets **107**, 791 (2006).
[34] M. Rudigier, K. Nomura, M. Dannhoff, R-B. Gerst, J. Jolie, N. Saed-Samii, S. Stegemann, J-M. Régis, L. M. Robledo, R. Rodríguez-Guzmán, A. Blazhev, Ch. Fransen, N. Warr, and K. O. Zell, Phys. Rev. C **91**, 044301 (2015).
[35] V. Werner, N. Cooper, J. M. Régis, M. Rudigier, E. Williams, J. Jolie, R. B. Cakirli, R. F. Casten, T. Ahn, V. Anagnostatou, Z. Berant, M. Bonett-Matiz, M. Elvers, A. Heinz, G. Ilie, D. Radeck, D. Savran, and M. K. Smith, Phys. Rev. C **93**, 034323 (2016).